Tones for Real: Managing Multipath in Underwater Acoustic Wakeup

Affan A. Syed
USC/ISI and National University of Computer and Emerging Sciences (NUCES)
affan.syed@nu.edu.pk
and
John Heidemann
USC/ISI
johnh@isi.edu
and
Wei Ye
Broadcom Corporation
weiye@broadcom.com

The principles of sensor networks—low-power, wireless, in-situ sensing with many inexpensive sensors—are only recently penetrating into underwater research. Acoustic communication is best suited for underwater communication, with much lower attenuation than RF, but acoustic propagation is five orders-of-magnitude slower than RF, so propagation times stretch to hundreds of milliseconds. Low-power wakeup tones are present in new underwater acoustic modems, and when added to applications and MAC protocols they reduce energy consumption wasted on idle listening. Unfortunately, underwater acoustic tones suffer from *self-multipath*—echoes unique to the latency that can completely defeat their protocol advantages. We introduce *Self-Reflection Tone Learning* (SRTL), a novel approach where nodes use Bayesian techniques to address interference by learning to discriminate self-reflections from noise and independent communication. We present detailed experiments using an acoustic modem in controlled and uncontrolled, in-air and underwater environments. These experiments demonstrate that SRTL's knowledge corresponds to physical-world predictions, that it can cope with underwater noise and reasonable levels of artificial noise, and that it can track a changing multi-path environment. Simulations confirm that these real-world experiments generalize over a wide range of conditions.

Categories and Subject Descriptors: C.2.1 [**Computer-Communication networks**]: Network Architecture and Design—*Wireless communication*

General Terms: Sensor Network
Additional Key Words and Phrases: Acoustic networks, Underwater sensor networks, Bayesian learning

This research is partially supported by the National Science Foundation (NSF) under the grant NeTS-NOSS-0435517 as the SNUSE project and grant number CNS-0708946, "Open Research Testbed for Underwater Ad Hoc and Sensor Networks", and by Chevron Co. through USC Center for Interactive Smart Oilfield Technologies (CiSoft).

1. INTRODUCTION

Sensornets are transforming for science and industry by enabling pervasive, in-situ sensing through inexpensive, wireless sensors. Their success has sparked interest in bringing these characteristics underwater to improve our ability to chart the oceans, lakes, and waterways that strongly influence our environment and can provide natural resources [Vasilescu et al. 2005; Partan et al. 2006; Heidemann et al. 2006].

Perhaps the most significant to changes when deploying sensornets underwater is the use of acoustic instead of radio-frequency-based (RF) communication. Radio communication is significantly attenuated underwater, and while optical links can provide high-speed communication over short-range, point-to-point links, they require careful aiming and so cannot fulfill the need for easy deployment as is possible with surface sensornets.

Underwater acoustic communication poses several challenges. The most serious is large propagation delays. With the speed of sound around 1500m/s underwater, and ranges of 0.1 to 10km, delays of 100ms are common and multiple seconds are possible. The large delay makes adapting traditional media access protocols difficult, since channel sensing time follows propagation delay, a simple CSMA MAC will consume a great deal of power listening to an idle channel. In addition, the underwater channel poses additional challenges, including temperature-based delays, ducting and significant problems due to multi-path interference. Several papers summarize these challenges [Catipovic 1990; Stojanovic 2003; Preisig 2006]

Since energy is a constraint in many underwater networks (for example, stationary networks, or battery powered gliders), some modems employ special wake-up tones and low-power wakeup receivers to activate modems [Benthos, Inc. ; Wills et al. 2006]. The use of tones (detecting energy on a channel), instead of a control packet, can reduce energy consumption of coordination. These energy savings occur because detection can be quick, as seen in low-power listening with radios [El-Hoiydi and Decotignie 2004; Polastre et al. 2004], and dedicated hardware can carry out detection with very little power, as seen in radio-based pagers and recent underwater modems [Wills et al. 2006; Schurgers et al. 2002]. Recent work has shown how to integrate tones into low-power MAC protocols, for broadcast [Mirza et al. 2009] and contention resolution [Syed et al. 2008]. Tone-based wakeup is also important for wakeup after long-duration sleep [Li et al. 2006], or triggering more sophisticated data reception algorithm [Benthos, Inc. ; Freitag et al. 2005; Wills et al. 2006; Schurgers et al. 2002].

Multipath interference is a problem in all wireless communication. For data, it causes inter-symbol or inter-chip interference. These problems have been extensively studied in radios [Price and Green 1958; Kuperman et al. 1998]. Long propagation makes multipath worse underwater, and only in the 1990s was coherent communication demonstrated underwater [Stojanovic et al. 1994]; managing data multipath is still an area of research [Song et al. 2007].

When tones are used for coordination, reflections from stationary objects cause the transmitter to hear echoes or *self-reflections* of their tones. More concretely, just like multipath-caused inter-symbol-interference (ISI) at a receiver, echoes cause tone *self-multipath* when tones are used in protocol level coordination. This paper is

the first to identify the problem of self-multipath for low-power underwater acoustic communication and we illustrate its impact on T-Lohi MAC protocol as an example (Section 2). In Section 3.2, we later discuss why other alternatives to using binary tones that help identify self-multipath are not viable due increased complexity and energy consumption.

The challenge of self-multipath is that a transmitter will always interfere with itself. We show that this challenge provides the means to address the problem: senders can and must *learn their self-multipath patterns*. This goal is difficult because of the unique challenges of underwater sensornets. First, current data-focused multi-path techniques do not directly apply because we are concerned with self-multipath, not sender-receiver multipath. In addition, the constraints of low-cost and low-power receivers require implementation of wakeup tones with simple signals; these constraints make sophisticated coding untenable. Finally we must allow for long acoustic propagation times and reflections to hundreds of milliseconds. In Section 3 we describe *Self-Reflection Tone Learning* (SRTL) where we use Bayesian techniques to learn the channel state using low-power acoustic wake-up hardware. In addition to directly applying to underwater MAC protocols, SRTL's ability to estimate the number of reflecting surfaces in the environment also indicates the sparsity of the channel. This information may assist optimizations that exploit sparsity in managing the complexity of multipath in data reception [Li and Preisig 2007].

Since wireless channels are very difficult to model or simulate, in Section 4 we demonstrate the effectiveness of our approach with experiments using an acoustic modem in three different physical environments. We establish that what SRTL learns matches to physical-world predictions through tests in a completely controlled anechoic chamber (Section 4.2). We show that SRTL copes both with reasonable (on average two spurious detections per sample) amounts of artificial noise through in-air experiment, and real underwater noise in a marina (Section 4.3). Furthermore, our underwater experiments show large temporal variation (changes within seconds) of the underlying reflection structure. Finally, we show that SRTL can track these changes to the environment (Section 4.4), and how environmental parameters and their estimates affect the accuracy of algorithm (Section 5).

The contributions of this paper are to identify self-reflections as a new problem posed in low-power, high-latency underwater communication; to show how Bayesian learning with SRTL can mitigate this problem on low-cost and -power hardware; and finally to show that it works experimentally in an underwater scenario. We believe this approach will be essential to energy conserving underwater media access protocols, and also useful for long-duration sleep, and may apply to the broader problem of multipath in high-latency channels. We have previously outlined the problem of self-reflection and potential solutions in a poster abstract [Syed et al. 2010]; this paper provides a more complete view of the problem and solutions with simulations and experiments.

2. PROTOCOL PROBLEMS RESULTING FROM SELF-MULTIPATH

While problems of multipath interference are well known, we next explore the negative results of *self*-multipath on network protocols. Self-multipath can cause prob-

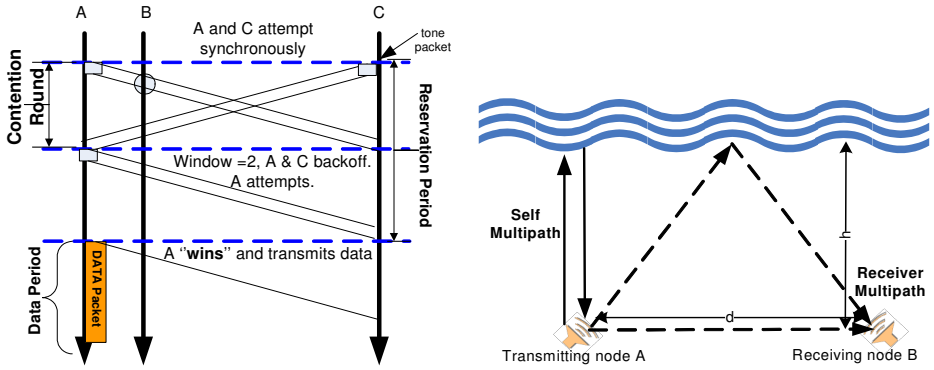

(a) An example T-Lohi protocol contention exchange

(b) Self-multipath of tones

Fig. 1. Explaining T-Lohi and the impact of tone reflection on the protocol. Reflections prevent vanilla T-Lohi from transmitting data, even with no contention.

lems in any protocol that uses tones, including T-Lohi [Syed et al. 2008], fast-boot from long-duration sleep [Li et al. 2006], and tone-based broadcast MAC protocols [Mirza et al. 2009]. As a concrete example, here we focus on Tone-Lohi (T-Lohi), a tone-contention-based MAC protocol [Syed et al. 2008], to show the failings caused by tone self-multipath.

2.1 Overview of T-Lohi

The key features of T-Lohi are that all contention is done with short wake-up tones, that can be observed with sub-mW energy consumption [Wills et al. 2006] and that it converges quickly due to accurate estimates of the number of contenders [Syed et al. 2008]. As a result, overall energy consumption is minimal even in the face of contention periods that may last up to a second. A full description of T-Lohi can be found elsewhere [Syed et al. 2008]; we summarize it here to show how tones are key to its energy-efficient operation.

In T-Lohi, nodes contend to reserve the channel to send data. It requires that nodes first send a *short tone* and then listen for the duration of the *contention round* to decide if reservation is successful. If only one node contends in a contention round, it wins, ending the *reservation period* and then transmitting its data. When nodes detect another concurrent tone, they interpret it as another node's contention and extend the reservation period by randomly backing-off. As tones are short and distributed over a long contention round (due to space-time uncertainty in high-latency communication [Syed et al. 2007]) each contender can do *contender counting* by counting the tones received. This count gives a good estimate of the number of other contenders, allowing the channel to quickly converge by adapting back-off in proportion to the number of contenders. Figure 1(a) shows an example of this process: nodes A and C have data to transmit but first send tones indicating contention. At the end of the first contention round both A and C have a count of two and back-off to attempt uniformly in one of the next *two* rounds. If no other tone is detected in a given round (like A does not in round two), collision free data

transmission occurs in the subsequent round.

Three significant sources of energy consumption in media access are idle listening, collisions, and control overhead [Ye et al. 2004]. T-Lohi addresses these sources of waste with two different mechanisms. First, in lightly used networks such as many sensornets, the majority of time is spent waiting for traffic, or idle listening [Ye et al. 2004]. Terrestrial sensornets have reduced this cost with scheduling [Ye et al. 2004] and low-power listening [El-Hoiydi and Decotignie 2004; Polastre et al. 2004]. In T-Lohi, we exploit very-low power dedicated hardware for tone reception, where tone listening consumes only 500μW [Wills et al. 2006], Second, to reduce the cost of collisions and control overhead, T-Lohi converges very quickly to a collision free channel reservation when traffic occurs. Quick convergence is possible because of contender counting, allowing the MAC protocol to converge in a small constant number of rounds with high probability, instead of the $O(\log n)$ convergence from binary-exponential backoff (as in Ethernet and 802.11).

2.2 Impact of Multipath

We now show how tone echoes result in self-multipath that cripples the T-Lohi protocol.

Figure 1(b) shows multipath occurring between two contenders, A and B. A tone sent by A reaches B directly and, a little later, via a surface reflection. This regular (receiver) multipath will cause multiple tones to be detected at B increasing B's contention counts. Although the throughput decreases due to slightly longer duration before a packet is sent, as T-Lohi converges time to data transmission is almost independent of density, T-Lohi will successfully contend the medium to send data. On the other hand A's echoes interferes fatally in its understanding of the contention status, and causes *self-multipath* (Figure 1(b)). As opposed to traditional multipath that results in data interference at receivers, self-multipath is essentially echo-interference amplified in the acoustic channel due to large propagation delays.

This self-multipath breaks T-Lohi MAC in such a way that contending nodes are *never* able to transmit data. This is because a *self-reflection* [1] for a contention tone sent in any contention round will result in an echo-induced tone detection. Since contenders transmit data in T-Lohi only when no other tone is detected, even a single reflecting surface, results in a contender *always* hearing an echo tone that it interprets as another contender. Thus a contender will always backoff and never be able to transmit data.

While one could work around this problem, perhaps by timing out after non-convergence, or by sending information with the tone, these approaches would increase energy consumption. Instead, we next show how Bayesian techniques allow contenders to *learn* about self-reflections, then choose to *ignore* them while remaining within the limitations imposed by a cost and energy-efficient wakeup tone receiver.

[1] We refer to each echo as self-reflection, distinct from the broader protocol-interference concept of self-multipath.

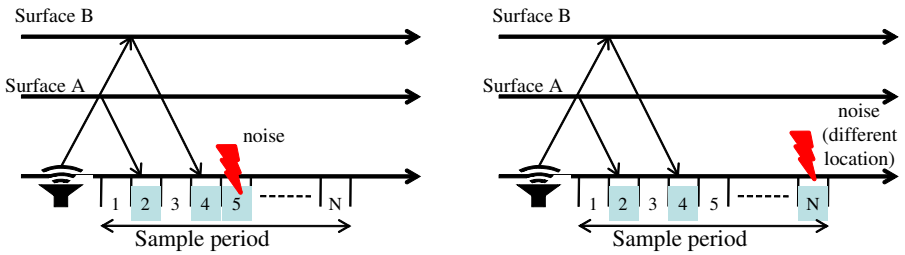

(a) First Sample: Two echo and one noise-triggered tone detection.

(b) Subsequent Sample: Echo locations repeat, but noise at different location.

Fig. 2. Key idea for SRTL algorithm: tone echoes after transmission repeat with same delay (or in discrete bins) but non-echo detections do not.

3. SRTL: LEARNING TO IGNORE ECHOS

We now introduce the Self-Reflection Tone Learning (SRTL) algorithm, our approach to manage self-reflection. We first give an overview of SRTL, then review Bayesian learning, the theory we draw upon (Section 3.3). We then cover SRTL details: what it observes about the channel, sources of error in those observations, and how these factors come together.

3.1 Overview of SRTL

The goal of SRTL is to learn about self-reflection and allow higher-level protocols (such as T-Lohi) to distinguish between echoes, random background noise, and tones sent for protocol-level coordination.

The key intuition behind SRTL is that echo time is *deterministic and repeatable* relative to a transmission, while noise and tones from other senders are independent and uncorrelated. An example of this observation is shown in Figure 2. Whenever transmitter sends a tone, it receives echoes from reflective surfaces (A and B in Figure 2) with a consistent delay. The tone receiver can also trigger in response to ambient noise (shown as bolts in Figure 2), or other transmitters, but these triggers occur *independently* of transmission times (compare location in Figure 2(a) and 2(b)). SRTL can therefore use this feature to learn and distinguish echoes from other tone triggers.

SRTL makes two assumptions: echoes are repeatable (over a short time period), and other triggers are independent. Since echoes are dependent on the physical placement of nodes and reflecting surfaces, they will be repeatable in a static environment. We confirm both of these assumptions, showing in Section 4.2 that the echoes we observe correspond directly with the physical environment. We tolerate minor variation in echo delay by discretizing responses into bins; in Section 5.3 we show our choice of bin size is reasonable and that we tolerate responses on bin edges. To manage changes in echos over time, we relax our our assumption of a for static environment in two ways. Over short time scales we use discrete bins (a 3ms bin can handle variation due to wave heights of 2.5m) to handle jitter (for example, due to tides). Over longer time scales, our experiments show (Section 4.4) that SRTL accommodates change due to drift or movement, adapting to a change in 3

to 48 samples (Table III).

The second assumption is that other (than echoes, for example from other T-Lohi contenders) tone triggers are independent of local transmissions. In other words, we assume random noise and asynchronous transmission of tones. Most observations confirm that underwater noise is uncorrelated and random [Catipovic 1990; Stojanovic 2003]; we also confirm this observation with experiments at the Marina del Rey harbor. It is possible that higher-level protocols or applications would create synchronization, either intentionally or accidentally [Floyd and Jacobson 1994]. However, typically MAC protocols explicitly randomize transmissions to eliminate deterministic synchronization caused by MAC or higher-layer protocols.

It is possible that higher-level protocols or applications would create synchronization, either intentionally or accidentally [Floyd and Jacobson 1994]. While some variations of T-Lohi intentionally synchronize transmissions similar to slotted ALOHA, MAC protocols in general can explicitly randomize transmissions to guarantee protocol-level synchronization does not occur, and thus concurrent application-level transmissions (by, say, an event trigger) are desynchronized at the MAC-level.

3.2 Alternate Approaches

Other approaches to tone identification are possible in addition to learning about echos. We consider related work in detail in Section 6; here we focus on two alternate approaches that use signal processing or coding techniques to disambiguate echoes from transmitted tones. For example, Rake receivers handle data multipath [Price and Green 1958] using chip-correlations, but because its complexity is proportional to delay, it doesn't easily scale to high-latency acoustic communication. Similarly Girod and Estrin use a similar approach for acoustic localization [Girod and Estrin 2001]. Coding sender identification in a data packet can also solve the issue of self-multipath. Alternatively, we could use time-based codes, pulsing the tone on and off. Frequency-based schemes are an area of potential future work (Section 7).

Most such schemes, directly or indirectly, reduce or eliminate the energy benefit of tone wake-up. To reach low power (0.5mW), low-cost operation, tone wake-up circuits use simple electronics and employ long activation times (up to 5ms) to maximize sensitivity [Wills et al. 2006]. Implementing signal processing or coding techniques on top of such hardware would require continuous, and therefore energy-inefficient, operation. For comparison, reception of just a single data byte, at 80b/s and receive power of 180mW [Freitag et al. 2005], requires 180mJ, compared our hardware's ability to detect a 5ms tone with only 1.5μJ [Wills et al. 2006]. Thus the cost of use of full data for signaling relative to binary tones is *five* orders-of-magnitude in energy consumption.

Alternate techniques also minimize the ability to detect and count contenders, as tones need to be of longer duration (to carry more than binary information), thus loosing the biggest advantage of tone-based protocol coordination. Thus, application requirements to minimize energy consumption preclude alternate approaches. We therefore turn to learning, and next provide background about Bayesian inference as employed by SRTL.

3.3 Bayesian Inference Background

Bayesian Inference is a well established approach that measures a probabilistic belief or knowledge regarding an event or hypothesis [Jaynes 2003]. We next briefly introduce the Bayes' theorem and show how it can be extended to perform inference based on empirically collected data.

The classical Bayes' theorem as defined for a bimodal hypothesis H, incorporating current evidence X is:

$$P(H|X) = \frac{P(X|H)P(H)}{P(X|H)P(H) + P(X|\overline{H})P(\overline{H})} \tag{1}$$

We assume, in all cases, either the hypothesis holds (H) or is not true ($\overline{H}$). The *prior probability*, $P(H)$ is the confidence before considering evidence X, while $P(H|X)$ is the confidence after incorporating this evidence. $P(X|H)$ is likelihood that event X occurs when hypothesis H is true, while $P(X|\overline{H})$ is likelihood X occurs even though the hypothesis is *not* true.

The Bayes theorem describes how a single observation modifies a belief. We build on localization work in robotics where successive observations allow robots to learn environmental features [Thrun 1998]. Observations of landmarks represent evidence increasing belief in the current location; manipulation and movement change the environment and decrease belief. Changes in belief are scaled by models of accuracy of sensing and actuation. Next, we describe how SRTL "senses" echoes, and how we model its accuracy to scale the belief update, thus learning echo locations.

3.4 Sampling in SRTL

To apply Bayesian reasoning, inspired by work in robotics, we must decide how to sense the environment, and how our samples correspond to our hypothesis. Thus, each time we send a tone, we keep track of any ensuing tone detections for a fixed duration, the *sampling period* (as in Figure 2), until any additional echoes would be too faint to detect.

To manage observations, we divide the sampling period into fixed-duration *bins*. For each bin i, we track the hypothesis H representing belief that the i^{th} bin corresponds to a self-reflection; we call such bins self-reflection (SR) bins. After a transmission and the entire sampling period, we have an array of evidences, one evidence per bin. Each sample can take on two values, either E_i for a tone detection (possible echo), or $\overline{E_i}$ when no tone is detected in that bin.

Bayesian learning has a rich mathematical background for estimating hypothesis by incorporating empirical data. While we currently model static nodes, incremental Bayesian learning can also incorporate motion if an appropriate model is provided [Thrun 1998]. To handle mobility, coordination between localized neighboring nodes can provide sufficient information to track location of reflecting surfaces and thus modifying the belief distribution. Thus we believe that a Bayesian learning approach is appropriate for learning tone-echoes.

3.5 Modeling Truth and Observations

A transmitter's observation corresponds to four possible real-world events: true echo detection, true silence detection, Non-echo Detection (ND), and Tone Cancel-

lation (TC). The first two events represent accurate observations about the world by the transmitter. However, we model the next two events because they represent observation error that can influence our reasoning.

Non-echo detection corresponds to an incorrect observation where our tone detector triggers for reasons other than our echo. Channel noise is a common source of a *ND* event. It may also be caused by an uncoordinated, *valid tone transmission* from another node. We cannot distinguish between both types of non-echo detections, but our approach will filter both out, since both are effectively random sources of noise (see assumptions in Section 3.1). A second source of error is *Tone Cancellation*—when there is energy on the tone channel (from either an echo, noise, or even another tone) at a receiver, but channel noise or another tone destructively interferes and prevents tone detection. In these cases, we falsely identify silence. A similar effect of tone cancellation occurs when a tone vacillates between two bins due to a dynamic environment (as we study in Section 4.4).

We model the event *ND* and *TC* with parameters p_{nd} and p_{tc}. These parameters are, for a given hardware and physical environment, our best estimates of the probabilities of the corresponding events. We show in Section 5 that our algorithm tolerates a margin of error in these estimates, so they need not to be set exactly. However, SRTL responds more rapidly when the estimate is close to the actual probability of each event.

3.6 The SRTL Algorithm

We now apply Bayesian learning to our system. We apply our algorithm in parallel to the hypothesis H_i and $\overline{H_i}$ for each bin, using the samples array observed in each sample period. For simplicity we stop using the subscript and describe a single bin. We refer to E and $\overline{E}$ as positive and negative evidence of a tone activation in that bin. Each bin is initialized with an initial belief, $Bel(H)^{init}$, that is subsequently updated after each sample period. We next describe our algorithm's update equations and its decision threshold.

3.6.1 *Update for Negative Evidence.* We consider absence of a tone as negative evidence ($\overline{E}$) that indicates a bin does not receive echoes. We therefore update our estimate from Equation 1, replacing X with $\overline{E}$. Also, we replace the term $P(H|X)$ with $Bel(H)^{posterior}$ (belief after incrementally incorporating current evidence) and $P(H)$ with $Bel(H)^{prior}$ (current belief incorporating all prior evidence) to reflect the standard Bayesian inference terminology [Thrun 1998].

$$Bel(H)^{posterior} = \frac{P(\overline{E}|H)Bel(H)^{prior}}{P(\overline{E}|H)Bel(H)^{prior}+P(\overline{E}|\overline{H})Bel(\overline{H})^{prior}}$$

We next explore how this update equation for negative evidence is modeled using our parameters p_{nd} and p_{tc}.

$P(\overline{E}|H)$ is the conditional probability for the event when no tone is detected, given that we *know* there was energy in the tone channel from an echo. This event is essentially the failure of our tone detection hardware to be triggered in the presence of tone energy. Assuming that bin duration is small enough to allow only a single detection, such an event can happen only if the tone echo is canceled by noise or interference. Thus, we can now define $P(\overline{E}|H) \equiv p_{tc}$.

Table I. Payoff table used in determining decision threshold that maximizes payoff.

	Reality	
Decision	*SR bin*	*not a SR bin*
SR bin (Ignore tones)	10	2
not a SR bin (Count tones)	1	9

$P(\overline{E}|\overline{H})$ is the probability for the event when no tone is detected given that we know that no echo can occur in that bin. However, this knowledge does not rule out non-echo detections caused by noise or other transmitters. Thus the event can be described by the *union* of two disjoint events: no non-echo noise is detected (the $\overline{ND}$ event) union with the event that although wake-up-triggering noise could have been detected it was canceled (the $ND \bigcap TC$ event). Noting that the above events are disjoint, $P(\overline{E}|\overline{H}) \equiv (1 - p_{nd}) + p_{nd} \times p_{tc}$.

Using the above definitions the update equation for negative evidence becomes:

$$Bel(H)^{posterior} = \frac{p_{tc} Bel(H)^{prior}}{p_{tc} Bel(H)^{prior} + (p_{nd} p_{tc} + 1 - p_{nd}) Bel(\overline{H})^{prior}} \tag{2}$$

This update is applied to our current belief $Bel(H)^{prior}$ to realize a new belief $Bel(H)^{posterior}$ when no tone is detected within that bin (negative evidence).

3.6.2 *Update for Positive Evidence.* Tone detection, E, is considered positive evidence of a bin being a SR bin. Similar to the negative update, we update our belief according to Equation 1, replacing E for the update event X. We next define the components of the update equation for positive evidence based on p_{nd} and p_{tc}.

$P(E|H)$ is the conditional probability for the event that tone detection occurs in a bin with known self-reflection. This probability is simply the complement of $P(\overline{E}|H)$; Thus, $P(E|H) \equiv 1 - p_{tc}$.

On the other hand, $P(E|\overline{H})$ is the conditional probability for a detection occurring in a bin we know has no echoes. This detection can, therefore, occur only because of wake-up-triggering noise (ambient noise and other contention tones) that is *not* canceled; the event $ND \bigcap \overline{TC}$. Thus, $P(E|\overline{H}) \equiv p_{nd}(1 - p_{tc})$.

Finally, using the above definitions the update equation for positive evidence becomes:

$$Bel(H)^{posterior} = \frac{(1 - p_{tc}) Bel(H)^{prior}}{(1 - p_{tc}) Bel(H)^{prior} + (p_{nd}(1 - p_{tc})) Bel(\overline{H})^{prior}} \tag{3}$$

This update is applied to our current belief $Bel(H)^{prior}$ to realize a new belief $Bel(H)^{posterior}$ when a tone is detected within a bin (positive evidence).

While Bayes works as described in theory, in our experiments we observed that long runs of consistent evidence would saturate the bins with perfect positive or negative belief ($Bel(H) = 1$ or $Bel(H) = 0$). We expect saturation occurs because of floating point rounding error. These equations are unable to shift from certainty, even in the face of later contrary evidence. We therefore cap the belief for each bin at a maximum value of 0.999 and a minimum value of 0.0001 to avoid saturation.

Table II. Research questions asked about the merits of our Bayesian learning algorithm.

		Environment		
Questions asked about SRTL	**Section**	Controlled	Lab	Underwater
Correctly ID known surface?	4.2	Yes	n/a	n/a
Is robust to Noise?	4.3	Yes	Yes	Yes
Can handle dynamic environment?	4.4	Yes	n/a	Yes
How sensitive to parameters?	5.1	Yes	Yes	Yes
What's the impact of discrete bins?	5.3	Yes	n/a	n/a

3.6.3 *Identification of SR Bins.* We intend for SRTL to work continuously in the background of any tone-based protocol. In T-Lohi, for example, we automatically get one sensing period for each contention round, so SRTL can sample the environment without incurring any additional overhead. We translate these continuous observations into decisions using a threshold. We bias our estimates by the payoffs of correct or incorrect decisions, then select the decision threshold that will be most profitable. For the values given in Table I, we can derive a fixed threshold of 0.45. Thus if the $Bel_i(H)$ is greater than 0.45 we will consider that to be a SR bin. We use this threshold in our experiments. In principle, one could adapt these values to the environment.

3.6.4 *SRTL Implementation Details.* Our algorithm uses fixed size bins; bin granularity is one factor to the sensitivity of our algorithm. In practice, bin size is limited by hardware. As a lower bound, our micro-controller has a millisecond level clock granularity, and interrupt debouncing causes a 2ms delay between successive tone detections. We therefore set bin size conservatively at 3ms for our experiments.

Our algorithm is quite lightweight. Its run-time and memory requirements are $O(n)$, where n is the number of bins that need update after each sample For 3ms bin, our algorithm easily runs on mote-class devices with $n = 60$.

4. EXPERIMENTAL EVALUATION OF SRTL

We now evaluate SRTL through experiments, both in the controlled setting of an anechoic chamber and a less controlled open lab. Table II summarizes our research questions, but our overall goal here is to show that SRTL can successfully manage echoes. To do that, we first confirm SRTL's conclusions are justified by the physical environment (Section 4.2), and evaluate how to copes with different levels of noise (Section 4.3). Finally we verify that the algorithm adapts to changes in environment, either due to movement of the node or other objects (Section 4.4). We begin by summarizing our experimental methodology.

4.1 Experimental Methodology

We evaluate SRTL using our acoustic modem in three different environments: a controlled, anechoic chamber, a less controlled laboratory setting (both using in-air acoustics), and in-water tests at Marina del Rey. We next describe details in common to the three environments we report here, how they differ, and bounds on our ground truth.

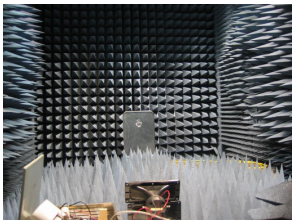

(a) Anechoic chamber experiments: in-air; single known reflecting surface as ground truth

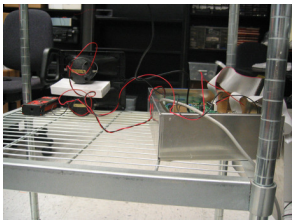

(b) Laboratory experiments: in-air; no ground truth

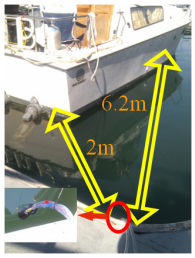

(c) Marina experiments: underwater; no ground truth

Fig. 3. Experimental setup at various location to answer the research questions posed in Table II.

4.1.1 *Details common to experiments.* We run experiments using the SNUSE acoustic modem [Wills et al. 2006], hardware revision 2. We use tweeters for in-air tests, and hydrophones when underwater. The modem is driven by a custom data collection program running on a Mica-2 mote. The microcontroller directly controls modem operation via I/O through a custom digital interface.

Each experiment consists of 200 sample periods of tone transmission followed by echo observation. For each sample, the mica2 configures the modem to transmit a wake-up tone, then switches to *tone-sleep* where it is quiescent until woken up by a tone. We timestamp each tone reception on the Mica-2 with 1ms resolution, then compute delay between initial transmission and echo. We later map detection delay into a corresponding 3ms bin (Section 3.6.4). Recall that these bins define the spatial sampling granularity for detecting echos (Section 3.4). The choice of 3ms is an engineering decision to manage the trade-off between the detection granularity and complexity. We later evaluate the impact of this bin size in detail (Section 5.3).

The SRTL algorithm currently runs in a host PC connected to Mica-2, allowing evaluation of SRTL response for the same underlying data set, although in principle it could run on the mote itself. After each transmission we record all tone triggers as positive evidence (E), and assume negative evidence ($\overline{E}$) for all other bins. We then update SRTL belief estimates based on Equations 2 and 3.

We set the sensing duration based on the maximum observed in-air range of our modem. We measure in-air range at 20m, so we anticipate reflections from objects up to 10m from the transmitter. We therefore anticipate echoes arriving with up to 60ms delay (20m, with speed of sound as 343m/s at 24° Celsius). We conservatively extend sensing duration to 100ms after each transmission.

We next describe details specific to our three experimental locations.

4.1.2 *Location-specific experimental details.* We carried out experiments at three locations, each providing us with different level of complexity in the reflective nature of the environment.

The first experiment location is an *anechoic chamber* at USC's UltraLab Laboratory. The chamber is designed to absorb all RF radiation for controlled radio experiments, but it also provides a good acoustically neutral environment. When necessary we place a large metallic pan in the chamber to act as a reflecting sur-

face (Figure 3(a)). We measure the distance from our transmitter as described in Section 4.1.3. Since the anechoic chamber is designed to be reflection free, this configuration lets us confirm against a strong ground truth: the physics of the measured location of our reflecting surface.

Our second environment is an *office laboratory* (Figure 3(b)). This location is much more complex, with multiple possible reflecting surfaces (walls, file cabinets, machine rack doors, etc.). We therefore observe more complicated channel response and so cannot provide firm ground truth. However, this more complex environment provides a richer level of noise and signal response.

For both in-air tests (anechoic chamber and laboratory), the modem uses high efficiency, Motorola piezoelectric tweeters that were impedance matched for both transmission and reception.

Our final experimental environment explores underwater performance. We test in the marina at Marina del Rey (Figure 3(c)). We use Benthos AT-18AT hydrophones as acoustic transducers that are optimal for our operating range of 17–19 kHz. Our samples were taken by dangling the hydrophone from the pier at 1m depth below surface (inset Figure 3(c)). The underwater environment provides little chance to estimate ground truth. However we observe several potential reflection surfaces nearby: Boat hulls, pier-wall, water surface, and Marina bottom. Our observations show deposit of large amounts of sediments and mud at the Marina bottom which make it a bad acoustic reflector. Similarly all reflection observed do not correspond to the water-surface (too close, reflections arrive before end of transmission) or pier-walls (too far, reflections die out before being received). We thus believe our reflection sources are nearby boat hulls with two identified reflection surfaces (shown with arrows in Figure 3(c)) at a distance of 6.2m and 2m.

4.1.3 *Estimating ground truth.* We estimate ground truth based on the physical distance between transmitter and reflector and compare this distance to measured echo distance (converted from measured echo delay). Both these measurements, however, have potential sources of error due to our modem hardware and the measurement process.

The largest source of error in measurement of echo delay is the detection circuit of our modem. We time-stamp the transmit time of tone and detection time of echoes to calculate the distance to reflector. Due to transmit side warm-up, the actual transmission time of the tone can vary by about 1ms. Similarly the actual detection time can vary by 2ms based on the strength of echo.

We measure the physical distance with a HILTI PD-40 high-precision laser range-finder. Accuracy is ±1mm, so we believe error in the distance measurement is minimal. However, the most significant source of error is in our measurement process when we approximate the angle for the line-of-sight measurement between the piezoelectric crystal located inside the transducer and the reflecting surface. This measurement error is approximately ±2cm and results in a corresponding delay error of about ±0.5ms (with speed of sound as 343m/s at 24° Celsius).

When comparing the ground truth to identified echoes, we have to reconcile the above independent errors, in both measured distance and echo location. In the figures, we show the tolerance region that accounts for the worst case error in each measurement. The identified location can safely be considered to match the ground

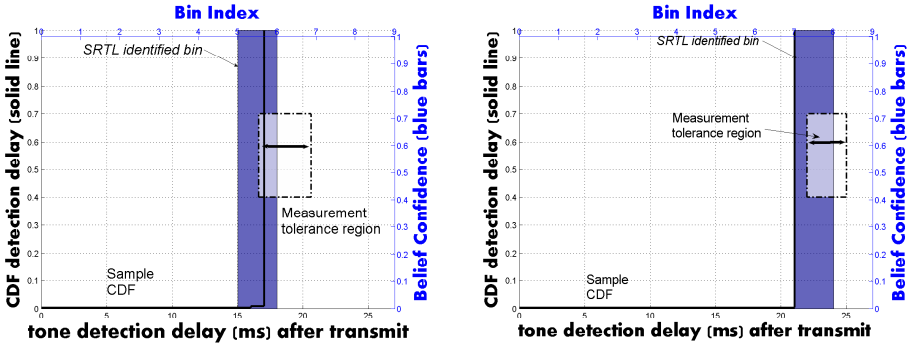

(a) Reflecting Surface at 3.36m (b) Reflecting Surface at 4.11m

Fig. 4. Experimental results showing the CDF of 200 samples and SRTL response with objects at known location, adjusted for measurement error (shown as the shaded area with dashed boundary).

truth if these regions overlap. Thus, due to the resulting overlap of the error bounds, the tolerance region varies on a case-to-case basis for each measurement.

4.2 SRTL Correctness

We first seek to confirm that SRTL can *correctly* identify the location of a known reflecting surface: does our algorithm and experimental setup match the physical configuration of the world?

Since this experiment needs knowledge of the ground-truth, we use the anechoic chamber to perform controlled experiments. For this experiment we place a reflecting surface perpendicular to the piezoelectric tweeters, measure its distance and compute the expected delay. We take several measurements (as described in Section 4.1) with the surface at a particular location. Since there is only one reflecting surface in the room, our algorithm should only identify the bin corresponding to the measured distance. We then compare SRTL's estimate with our prediction from the physical distance.

Figure 4 shows the result of our experiments for reflectors at two different distances. Each figure combines three different values: prediction from physics, all observations, and the SRTL belief distribution. The dotted box indicates the prediction from our distance measurements, including estimated error. The solid black line represents the cumulative distribution function of delay values for all the samples considered by SRTL, measured against the left axis. Finally, solid blue bars represents the belief distribution ($Bel_i(H)$) for each bin in the 100ms sensing period (we show only the first 25ms and omit the remainder since there is no belief there). Bin indices are given on the top axis.

Figure 4(a) shows the result of our experiment with the surface measured to be at 3.36m from the transmitter. The sample CDF shows that nearly all samples are received at a delay of 17ms, which corresponds to the fifth bin. SRTL is able to identify this bin with complete confidence and we can see that the identified bin lies within the error bounds of the physically measured surface location.

Figures 4(b) shows results from the same experiment with the surface at 4.11m (the seventh bin). We observe that the bin identified by SRTL matches the location

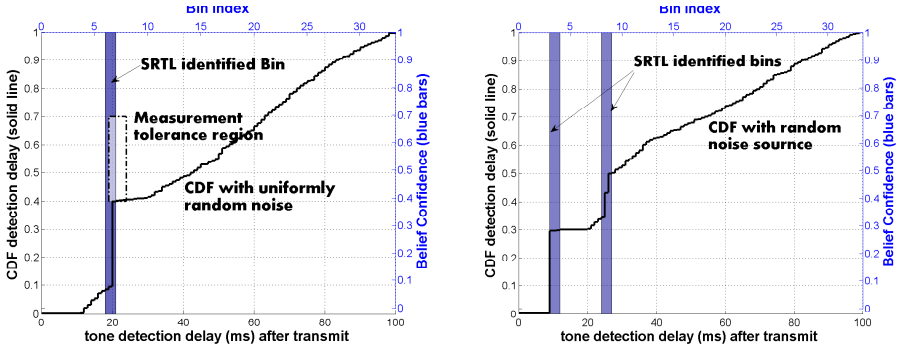

(a) Noise source, with ground truth.

(b) Noise source, with *no* ground truth.

Fig. 5. SRTL response for a noise source that produces on average two artificial detection for each SRTL sample.

indicated by the CDF and predicted by our range measurements.

From these experiments we conclude that we can completely explain SRTL performance under known conditions; SRTL places known reflections in their correct bin as predicted by the physical setup.

4.3 Robustness to Noise

Although we verified that SRTL works as expected in perfect conditions, we also care about performance in the face of environmental noise or additional, but unsynchronized (assumptions in Section 3.1), transmitters. We evaluate this aspect by first adding a controlled in-air noise source and then performing experiments in a naturally noisy underwater environment.

4.3.1 *In-air, Controlled Noise source.* We investigate this question by adding an artificial noise source to our experiments. This noise source is a second modem that transmits tones, triggering non-echo detections at our original sender (on which SRTL algorithm is running). Our artificial noise source transmits tones repeatedly, with inter-transmission times chosen uniformly randomly within a fixed interval. We then vary this interval to adjust the degree of noise, with smaller intervals causing greater (more frequent) noise. Since timing of noise is random, we expect SRTL to ignore such noise and still be able learn reflections from known surfaces. (We select this noise model to provide simple, controlled tests. Exploration of richer noise sources is an area of future work.) We perform our experiments with different levels of noise in both controlled and uncontrolled environments (with known and unknown ground truth).

Figure 5(a) shows the result for the controlled environment of the anechoic chamber. The presence of a gradual slope in the sample CDF (the solid black line) indicates the presence of noise. We looked at several noise levels, Figure 5(a) shows the case where there are, on average, two noise triggers in each sample period for the single true echo. However, SRTL identifies the correct bin of the reflector even with substantial interference as it can suppress the randomly distributed noise and learn the true echo locations. We conclude from this experiment that while SRTL

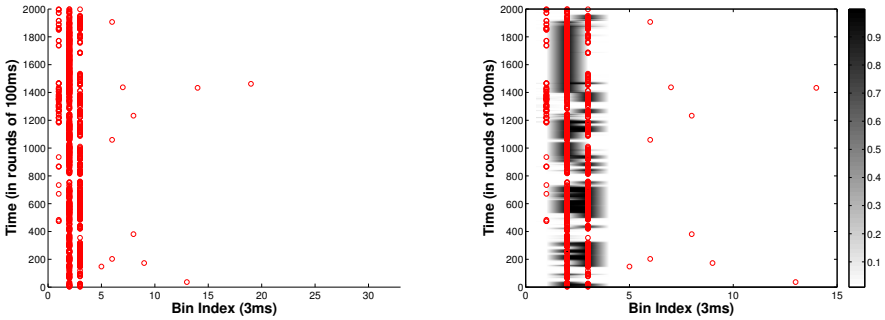

(a) Raw underwater noise and reflection structure.

(b) SRTL response to the tone transmission response structure.

Fig. 6. The structure of underwater tone-reflection and SRTL's (p_{nd}=0.5, p_{tc}=0.5) response. The figures are showing time-series of observation, each 100ms long, where each circle represents a detection and the SRTL confidence shown as a grayscale overlay.

will learn its environment, it will not be fooled by other tones (for contention in T-Lohi) or some levels of environmental noise.

Since an uncontrolled environment provides a richer, and more complex, multipath structure, we next reproduce this experiment in our lab where identification is more challenging for SRTL. Figure 5(b) shows the result of our experiments. Over many experiments with and without noise (not shown) SRTL detects two likely echoes in bins 4 and 8. Although we do not know the ground truth surface, these, and the CDF, empirically indicate the presence of two reflecting surfaces. Again, we see that the algorithm consistently identifies these two locations as self-reflection bins while suppressing random noise.

From the above results we conclude that SRTL can tolerate random noise up to at least two false triggers per sample period, and shows the need to further characterize the limits of noise tolerance. We do not characterize further due to hardware limitation, but explore greater noise tolerance using simulations in Section 5.2.

4.3.2 *Natural Underwater Noise in the Marina.* We anticipate that real-world noise and multipath will be more complex, so we next present experiments in an underwater environment where both the noise source and environment are uncontrolled. We first show the nature of reflection and noise in an underwater environment as specific for tone detection. We then show how SRTL responds to this manner of noise.

Underwater Reflection structure: Figure 6(a) shows the raw reflection and noise structure from an experiment performed at 1m depth. The x-axis shows bins, each with potential reflections or noise. Each bin is 3ms wide, a function of our minimum tone-detection time. The y-axis shows multiple rounds of transmissions, each 100ms apart. Thus the x-axis shows a snapshot of the environment due to a single transmission, while the y-axis shows how the environment changes over time.

This figure supports two observation about how the underwater reflection structure interacts with our algorithm. First, the reflections from surfaces can exhibit high temporal variability. This variability is evident in the response for the second

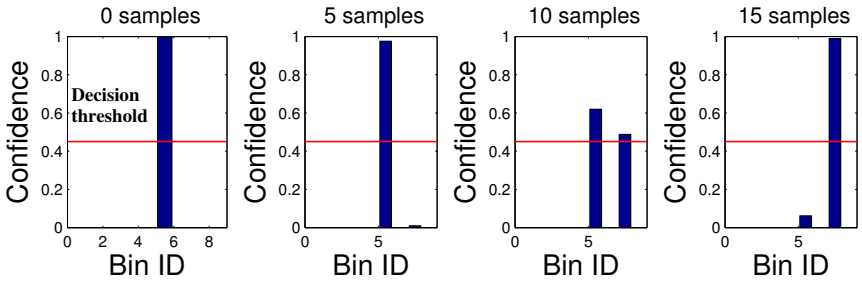

Fig. 7. SRTL (p_{nd}=0.4, p_{tc}=0.4) response to change in location of reflecting surface from 3.36m (bin 5) to 4.11m (bin 7).

and third bin (the vertical columns at $x = 2$ and 3). While these two bins have regular detections (frequent circles in either column), they also have several gaps with no detections (for example, at time 800 in both columns, at $y = 1600$ for bin 3). These epochs can last from a few sample rounds, to several 10s of these rounds that last several seconds. These gaps show evidence that reflections can vary over very small time scales

The second observation regards the nature of underwater noise and its effects on modeling of SRTL parameters. While the second and third bin show regular detection, there is a scatter of seemingly random detections at bins 5 through 20. We consider those detections to be noise. With this classification our modem detects just 11 noisy detections in over 2000 experiments (running the length of the y axis). Thus, for 3ms bin, we can compute a 0.00016 *tone error rate*. While this measurement is topically similar to our p_{nd} parameter, it excludes the notion of other transmitter that is central to SRTL.

SRTL's Response to Underwater Reflections: We now look at the response of SRTL to the temporally variable and noisy reflection structure in an underwater environment. Figure 6(b) shows this response as a grayscale overlay on our raw underwater data, indicating confidence that each bin is a reflection. We observe that the confidence of SRTL for each bin increases (becomes darker) in lock-step with the circles representing actual detections. Thus we see that SRTL is not only able to detect bins, but also roughly matches the temporal nature of the raw data. To get a better understanding of how SRTL responds to variable reflections we quantitatively analyze its response time in Section 5.1.

4.4 SRTL in a Changing Environment

Most underwater environment change, either due to tides or currents, precession on an anchor, or movement of human artifacts or fish. Since in the last section we argue that reflections show significant temporal variation, we next evaluate how well SRTL adapts to a changing environment. Properly configured, Bayesian learning can track changes in belief so we expect SRTL to track changes in the environment successfully.

4.4.1 *Controlled Experiment: Anechoic chamber.* To investigate SRTL response to environmental changes, we return to the anechoic chamber. We place a reflecting

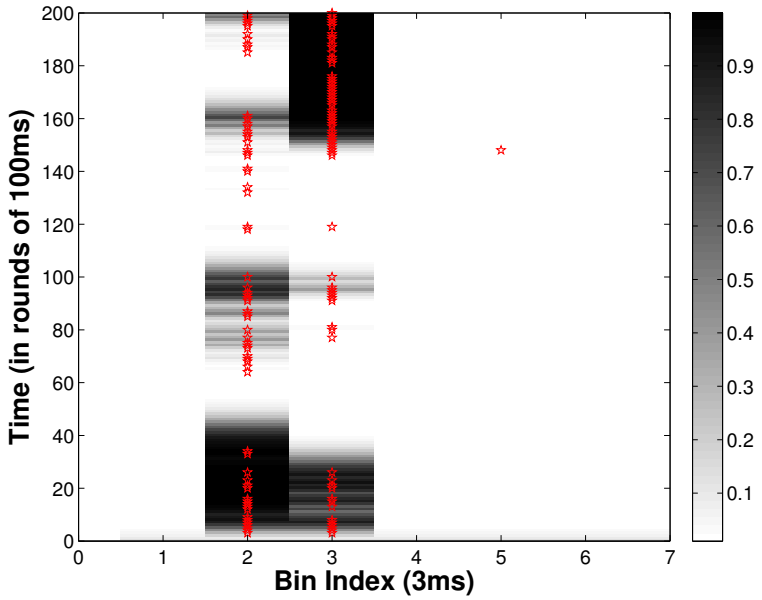

Fig. 8. SRTL adapting to temporal variability of underwater reflection structure. This figure magnifies a portion of Figure 6(b), replacing circles with stars for clarity. Whitespace in the figure represents SRTL not assigning importance to bins which lack echoes.

surface at a known location (at 3.32m, corresponding to the fifth bin). We then take twenty consecutive samples at that location to train the SRTL algorithm to identify that location with maximum confidence. We then move the reflecting surface to a different location (4.11m, corresponding to bin 7) relative to the transmitter. We then observe how SRTL's belief distribution (about which bins are SR) evolves as it collect additional observations. We expect SRTL to track the changed environment and identify the new bin after incorporating a few samples. The decision threshold is set using the mechanism described in Section 3.6.3.

Figure 7 shows how SRTL's belief changes as it takes more observations. Initially SRTL is certain that bin five is the surface, but after 5 samples (the second figure from the left), this believe begins to waver. At 10 samples it has begun recognizing bin 7, the new location, as a self-reflection, although it still remembers the old location. Finally, after about 15 samples, SRTL has nearly completely shifted its understanding of the environment. This experiment demonstrates that SRTL will adapt to changes in environment.

4.4.2 *Uncontrolled Underwater Experiments.* In the last section we showed that underwater reflections show large variability in time. This result validates the need for SRTL to adapt to changes in the environment. To understand SRTL adaptivity, we next zoom in to Figure 6(b).

Figure 8 shows the first 200 samples of our experiment. The magnified response clearly shows that when successive detections occur in a bin (*e.g.*, the continuous

Table III. Quantifying the rise and fall time (in number of observations) of SRTL.

	Parameter Settings (p_{nd}, p_{tc})					
	(0.2,0.2)	(0.2,0.7)	(0.7,0.2)	(0.5,0.5)	(0.5,0.7)	(0.7,0.5)
Rise-time (min-max)	6	6	26	14	14	26
Fall-time (max-min)	7	22	12	23	48	36
Rise-time (min-threshold)	3	3	13	7	7	13
Fall-time (max-threshold)	4	17	7	12	25	19

vertical column of dots for the first 10 samples for bin 2 and 3), SRTL quickly adapts and increases confidence (the overlay becomes darker). At the same time, successive samples without any detection (samples 40–60 for the second bin) leads to a gradual decrease in confidence (light colored to no overlay). Moreover, we observe the SRTL algorithm adapts to variability within successive samples (*e.g.*, between samples 60–100 for the second bin) and tracks the raw data by increasing or decreasing confidence (observe the variation in grayscale during that period). Thus we claim that SRTL adapts to the temporal variability of an underwater reflection structure. In the Section 5.1 we quantitatively characterize the response time of SRTL and its dependence on algorithm parameters.

5. SRTL PARAMETER SENSITIVITY

The previous section describes experiments that show SRTL works well, even with noise and environmental change. SRTL has several parameters that affect its operation, including estimates of *ND* and *TC* events and choice of bin size. While the previous section validated the accuracy and robustness of our algorithm, any real implementation needs to correctly understand how significant each parameter is to SRTL's accuracy and robustness. We next evaluate how sensitive SRTL is to choice of these parameters to provide guidelines that will help in any real deployment and use of the algorithm.

5.1 Estimates of Observation Errors

SRTL's learning algorithms takes two parameters, p_{nd} and p_{tc}, that are used to adapt its belief to new observations. In Section 3.5 we describe how these parameters model our estimates of observation errors. The Bayesian update equations completely depend on these two parameters. Thus these two parameters will have the largest impact on accuracy and response time of SRTL, both metric being of importance when defining the usability of our algorithm for echo-identification. To understand how the parameters affect SRTL, we first evaluate the response time of SRTL in a controlled but emulated setting. We then reexamine parameter setting in the more complex and uncontrolled underwater environment.

5.1.1 *Parameter Choices: Controlled Emulated Environment.* A quantitative measure of the impact of SRTL parameters allows us to better predict its behavior in a time-varying underwater channel, compared the intuition presented Section 4.3, For this purpose we first measure the algorithm's *rise-time* and *fall-time*, *i.e.* the number of observations to cross the decision threshold and reach minimum or maximum confidence, in either direction. These two metrics, along-with the behavior of

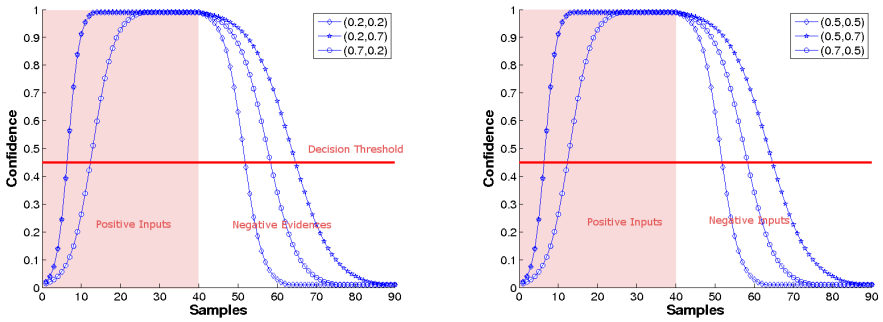

(a) Low parameter settings

(b) Medium parameter settings

Fig. 9. Confidence curves for SRTL showing the impact of parameters on its response time. We show SRTL response for 40 consecutive positive and then 40 negative inputs. The legend reads as $\{p_{nd}, p_{tc}\}$.

SRTL during these transitions, give us a quantitative measure of the impact each parameter has on SRTL's response. To measure these metrics we emulate a controlled environment by feeding SRTL an artificial reflection series, where the first 40 samples are positive in a specific bin. From this series we measure the rise-time of confidence. These are then followed by another 60 negative samples, causing SRTL to loose confidence and allowing us to measure the fall-time. Figure 9 shows the result of these experiments for three different combinations of parameters with low, medium and high values (0.2, 0.5, and 0.7). Table III quantifies the rise and fall time of SRTL for these parameter settings in number of observations.

We first look at the absolute value of the rise- and fall-time as these allow us to quantitatively understand the behavior of SRTL in a changing underwater environment. The first thing we observe is that the rise-time of SRTL depends solely on the p_{nd} parameter (the first and third row of Table III). This result is corroborated by the positive update Equation 3 which can be simplified to completely remove the p_{tc} parameter. On the other hand, the fall-time depends on both parameters (verified by Equation 2), but here p_{tc} has the greater influence. Thus (0.7, 0.5) requires 13 more samples than the 23 for (0.5, 0.5) fall time; compare that with 25 more samples needed for (0.5, 0.7). We conclude that high p_{tc} values act to damp the response of our algorithm to missed reflections, while large p_{nd} dampens response to new bins. At the end of next section we discuss the impact of these results, controlled experiments, and how these can inform setting SRTL parameters.

We can also understand the impact of parameters on SRTL's response to changes in environment by observing the rate-of-change, or slope, of the curves during rise or fall-time. The slope of these curves determines the stability of the confidence with time varying reflections. Thus, if at some confidence value a curve responds to a single positive evidence with a rise in confidence that is larger, in absolute terms, to the decrease for a single negative evidence (like (0.5, 0.5) and (0.2,0.2) cases), it requires fewer successive detections to maintain confidence. In the inverse case of a larger confidence drop than rise, (like the (0.7,0.2) case), a few missed detections can keep the confidence low.

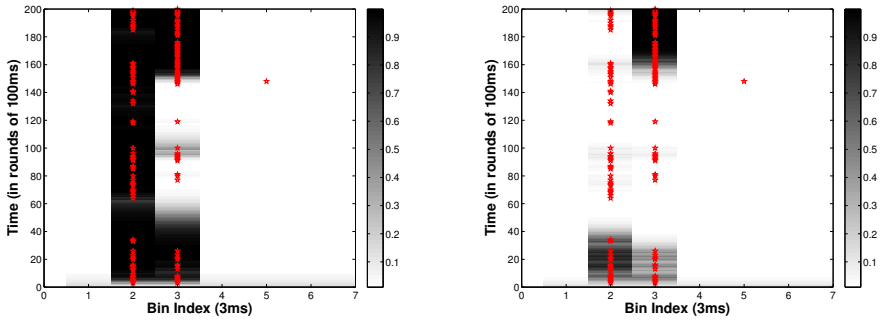

(a) p_{nd}=0.5, p_{tc}=0.7 (b) p_{nd}=0.7, p_{tc}=0.5

Fig. 10. Impact of parameter setting on SRTL response (as grayscale) for the same underwater reflection structure as shown in previous figures.

The slope of these curves allow us to reason about the choice of decision threshold. As these slope are asymmetric, with small values at low and high confidence ends but fairly sharp slope between 0.15 and 0.9. Such a behavior indicates that once the initial inertia is overcome, a few consistent observations can reach any decision threshold in the middle range. Thus, any decision threshold within the $[0.3, 0.7]$ confidence range (but not at either extremes) can be reached within 3—7 samples. We conclude that, for most practical thresholds, the accuracy of SRTL is marginally affected by the exact decision threshold.

Finally, detection theory allows one to trade certainty of detection for time; we observe this tradeoff in the value of parameters. Thus, a high value of p_{nd} confirms a new reflecting surface slowly, but also increases accuracy as we now do not react to spurious detections. A similar tradeoff in reacting to transient reflection-loss occurs for higher values of p_{tc}.

5.1.2 *Parameter Choices: Uncontrolled Underwater.* Our controlled experiments allow us to conclude that p_{nd} alone impacts the increase in confidence while p_{tc} has a more dominant impact on the decrease. We now want to see if these conclusions can shed light on the behavior of SRTL for an uncontrolled underwater environment.

For this purpose we look at SRTL's response to the raw data shown in Figure 6(a). Figure 10 shows its response for the first 200 samples (having large temporal variability) for two parameter settings, while Figure 8 shows result for a third setting of (0.5,0.5). We first observe the impact of p_{nd} by comparing Figure 10(b) ,with a higher p_{nd}=0.7, to Figure 10(a) with p_{nd}=0.5. We observe that even with the same reflection structure, Figure 10(b) never gains much confidence for bin 2 as a SR bin (between 0-40 samples), while Figure 10(a) does so consistently. This response is mostly explained by the conclusion from last section that a large p_{nd} damps the rise-time and requires more consecutive detections to cross the decision threshold.

A second observation is that between 40-60 samples, the confidence for bin 1 in Figure 10(a) does not decrease significantly even with no reflections arriving. We compare with Figure 8, where the confidence at the beginning of the range is similar, however by the 50^{th} sample it has minimal confidence. Again this result

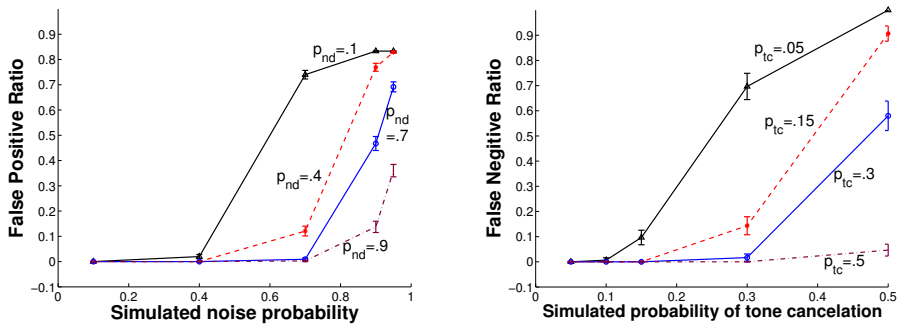

(a) False Positives (b) False Negatives

Fig. 11. Fraction of false positive and false negative as *simulated* noise and chosen noise estimates vary. Error bars show 95% confidence intervals.

is explained by our previous conclusion that a higher p_{tc} in Figure 10(a) damps the effect of missed reflections, thereby retaining the confidence in a particular bin longer.

Overall, we conclude that for use in T-Lohi where we prefer a false positive for a SR bin identification (to mitigate the chance of a transmission deadlock), a low value of p_{nd} and a higher value of p_{tc} allows us to detect a possible reflection surface quicker while also increasing the memory for that location. However, these values still need to carefully chosen as even in T-Lohi,as consistently ignoring actual contenders (a possibility with such parameter settings and a few false positives) will lead to packet collision. Of course, different applications (than T-Lohi) will have different preference for parameter settings.

5.2 Parameter Alignment with Environmental Conditions

Hardware limitations prevent us from introducing large amounts of non-echo or tone cancellation noise in these experiments. To study both types of noise, we simulate the algorithm with artificial noise, allowing us to explore arbitrarily high noise levels under controlled conditions. Our goal is to understand what levels of noise cause SRTL to fail, and how SRTL behaves when our noise estimates (p_{nd} and p_{tc}) differ from the actual amount of noise.

To observe false positives, we vary simulated (wake-up tone triggering) noise in the environment. In Figure 11(a) we fix both the simulated and algorithm parameters of tone cancellation probability at 0.05, we then vary noise (the x-axis) and observe the fraction of false identifications for different values of p_{nd}. Figure 11(a) shows that the fraction of incorrectly identified bins increases as the simulated environmental noise increases. However, the exact rate is a function of our noise estimate p_{nd}, with larger estimates making SRTL more skeptical that tone-triggers indicate self-reflections, thus reducing the number of false positives. Thus, with $p_{nd} = 0.4$, 70% simulated noise (the second line from the left) leads to just 0.11 faction of false positives, but an estimate $p_{nd} = 0.7$, gives nearly no false positives at the same simulated noise level. In general, SRTL performs reasonably as long as the estimate is at least as large as true noise, with some leeway when

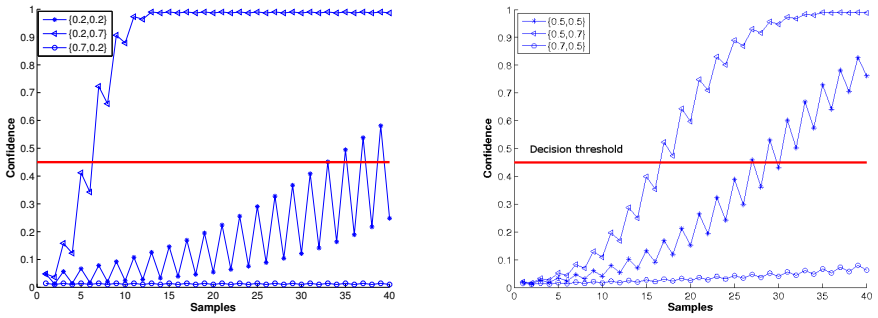

(a) Low parameter settings

(b) Medium parameter settings

Fig. 12. An effect of discrete bins is for reflections at boundaries might fall in either bins. We consider the worst-case where alternate samples fall in adjacent bins.

noise is low.

To observe false negatives we vary the simulated probability of a tone cancellation. In Figure 11(b) we fix both the simulated and algorithm input values of noise detection probability at 0.4. Figure 11(b) shows that the fraction of SR bins that are SRTL fail to identify (false negative) increases with the simulated tone cancellation probability. Just as with false positives, performance is best when the estimate (p_{tc}) is close to actual tone cancellation probability, but at low levels SRTL will tolerate noise two or three times that estimate. The main difference is that SRTL is less forgiving of tone cancellation than noise. Because there are few echoes, moderate cancellation makes them difficult to identify. Fortunately, as it is rarer for interference to completely suppress channel energy, so cancellation is rarer than non-echo noise.

Thus we conclude that SRTL can tolerate a wide range of noise in the environment, provided that corresponding estimates (both p_{tc} and p_{nd}) are reasonable approximations. Moreover, over-estimating the actual observation errors has a lesser penalty than under-estimating these parameters.

5.3 Impact of Bin Discretization

SRTL uses discrete bins to track belief and provide efficient and low-complexity operation even on mote-class devices. Our final question is to explore how bin size affects our algorithm. We have three concerns: bins that are too small may disperse observations, bins too large may cause echoes to hide real tones from other transmitters, and even with correctly sized bins, tones might fall on the border between two bins. Our observations about system sensitivity (Section 3.6.4) limit our bins to at least 3ms, and even with our underwater experiment we have not observed drift by more than a few ms, thus we believe this bin size is appropriate. We next look at echoes that lie at bin-borders to investigate the worst case impact of using such a low-complexity, low-memory implementation.

For a reflecting surface exactly on the edge of two bins, minor observation jitter (hardware delays, software locks, clock granularity, or simply very slight motion of either the node or reflecting object) can easily move observations in either di-

rection. To simplify evaluation, we consider the worst case scenario: each sample produces detection at an alternate of two adjacent bins. We emulate this scenario by artificially providing such a sample input to our SRTL algorithm.

Since the bins see equivalent observations (modulo a two sample period), belief in each bin is identical. Figure 12 plots the belief in one of the adjacent bins as more samples are incorporated by the algorithm. We see that combining a low value of tone cancellation probability with a higher value of noise detection, the (0.7,0.2) and (0.7,0.5) tuples, makes it unlikely for either bin to be identified as reflection. This result is because low value of p_{tc} implies any confidence is lost quickly, while a higher value of p_{nd} requires long time for new identification to be made. This result is also supported from our observation about the slope of confidence curves in Section 5.1 as the change for a positive evidence is easily offset by these parameter settings.

However, by choosing parameters that increase the memory of location (higher p_{tc}) and have more agile response to detection (lower p_{nd}), results in a rise in the confidence for each bin. The rate of this change is, again, dictated by the parameter values. Thus, equal parameter, like (0.5,0.5) and (0.2,0.2), result in a gradual increase as the positive agility of p_{nd} is nearly equally (but not completely, as discussed in Section 5.1) balanced by the damping of p_{tc}. A larger imbalance, in the case of (0.7,0.5) and (0.7, 0.5), leads to a much faster rise in confidence, respectively taking 17 and 7 samples to cross the decision threshold.

The SRTL input parameters, therefore, provide us with a fine-tuning-knob to adapt our algorithm to the need of our environment. As we argued before (at the end of Section 5.1), these parameters should be set based on the required accuracy (in false positives and negatives) of the application using SRTL. Our analysis here provides guidance to set these parameters.

6. RELATED WORK

Our work on tone self-multipath is related to three areas: data multipath, echo-detection techniques, and Bayesian learning. We next describe background for each related area and highlight the novelty of our approach.

Combating the large multipath spread to achieve robust data communication is considered the most challenging task of an underwater acoustic (UWA) communication system [Stojanovic 1996; Catipovic 1990]. Coherent systems, bandwidth efficient for the band-limited UWA channel, are much more sensitive (than non-coherent systems) to this large multipath spread which can result in inter-symbol or inter-chip interference. Stojanovic et al. were the first to propose a suboptimal, and therefore less complex, Decision Feedback Equalizer (DFE) jointly optimized with a Phased Locked Loop (PLL) that enabled coherent underwater communication [Stojanovic et al. 1994]. Recently Time-Reversal-Mirror (TRM) has also been considered as a mechanism to handle multipath in an underwater environment [Song et al. 2007]. Such existing physical-layer techniques, including Rake receiver [Price and Green 1958] or TRM [Song et al. 2007], distinguish between several copies of the same signal at a *receiver*. However, we are faced with the challenge of *self-multipath*, where a transmitter must identify echoes of its own signal, while using low-power acoustic tones, not the more energy consuming data. We

therefore require different approaches at the transmitter.

Perhaps the closest to our work are acoustic signal processing techniques based on interpreting echoes from the environment, including echolocation, echo-sounding, and sonar [Knight et al. 1981; Hammerstad et al. 1993]. While sonar is used to detect the presence of obstacles for navigation [Knight et al. 1981], echo-sounder are widely deployed for bathymetric data collection [Bourgeois et al. 1999]. In both active sonar and echo-sounding, sound pulses, often called "pings", are sent for echoes detection that measures the distance to a reflection surface. In these techniques signal correlation or matched filters are used to disambiguate echoes. Furthermore, sonar identifies targets by comparing echoes with pre-recorded signatures. However, such techniques are not designed for energy-efficient applications. Underwater sensornets use low-power, wake-up circuit that focus on energy and cost-efficiency. Thus the wake-up circuit is a simple analog part that precludes the use of any complex signal-processing techniques. Our work tackles this unique problem of echo identification for low-cost, low-power acoustic tone signals by using the simple tone activation signal provided by such devices to probe the medium and learn to accurately identify echoes.

Bayesian learning as a field builds upon the rich mathematical history of Bayesian statistics. Bayesian learning uses empirical data (collected by sensors) to progressively improve estimates of system parameters [Thrun 1998; Hertzmann 2004]. Researcher have used Bayesian inference to learn complex CGI (computer graphic imagery) models from human actors [Hertzmann 2004] as well as to localize robots using landmarks [Thrun 1998]. The problem of self-multipath is unique for low-power acoustic tone-based communications. We are the first to use Bayesian learning mechanism to overcome the impact of such tone echoes within the constraints of low-cost, energy-efficient hardware necessitated in underwater sensornets.

7. FUTURE WORK AND CONCLUSIONS

There are several possible future directions. Although we focus on Bayesian approaches, other possibly simpler approaches like exponential weighted moving averages, may also work. We plan to integrate our approach into T-Lohi and validate that SRTL provides a solution to problems described in Section 2.2. We believe our approach will work better in deep water where surface and bottom reflection are absent. However, since current experiments are in shallow water, verifying this claim requires future deepwater experiments. The approach also requires addition evaluation in rapidly changing conditions like rough weather; while we have shown in Section 4.4 that SRTL can adapt to change in environment, optimizing performance under rapid changes is an open question. Finally we can use SRTL to suppress receiver multipath of contention tones and explore using our algorithm in conjunction with other protocols for underwater sensornets, such as the tone-based broadcast mechanism proposed in TB-MAC [Mirza et al. 2009].

An orthogonal area of future work is to explore wakeup tones where each device is assigned a unique frequency. Such an approach simplifies the issue of tone reflection for protocol coordination, but raises new issues of the effects of frequency-varying attenuation on wakeup, as well as configuring and managing frequencies across very limited bandwidth.

In this paper we first identified the issue of tone self-multipath unique to the large propagation delays of acoustic networks. We then used T-Lohi as an example to show that this delay can significantly reduce the throughput of our MAC protocol. We then introduced a Bayesian learning algorithm, Self-Reflecting Tone Learning (SRTL), that can be used to learn-and-ignore these self-multipath or echo tones. We performed experiments to verify that our algorithm is correct, robust to noise, and can adapt to a dynamic environment.

REFERENCES

Benthos, Inc. *Fast And Reliable Access To Undersea Data.* `http://www.benthos.com/pdf/Modems/ModemBrochure.pdf`.

Bourgeois, B., Martinez, A., Alleman, P., Cheramie, J., and Gravley, J. 1999. Autonomous bathymetry survey system. *IEEE Journal of Oceanic Engineering 24,* 4 (Oct), 414–423.

Catipovic, J. Jul 1990. Performance limitations in underwater acoustic telemetry. *IEEE Journal of Oceanic Engineering 15,* 3, 205–216.

El-Hoiydi, A. and Decotignie, J.-D. 2004. WiseMAC: an ultra low power mac protocol for the downlink of infrastructure wireless sensor networks. In *Proceedings of the 9th IEEE Symposium on Computers and Communications*. IEEE Computer Society, Washington, DC, USA, 244–251.

Floyd, S. and Jacobson, V. 1994. The synchronization of periodic routing messages. *ACM/IEEE Transactions on Networking 2,* 2 (Apr.), 122–136.

Freitag, L., Grund, M., Singh, S., Partan, J., Koski, P., and Ball, K. 2005. The WHOI Micro-Modem: An acoustic communications and navigation system for multiple platforms. In *Proceedings of the MTS/IEEE Oceans Conference*. IEEE, Washington, DC, USA.

Girod, L. and Estrin, D. 2001. Robust range estimation using acoustic and multimodal sensing. In *Proceedings of the IEEE/RSJ International Conference on Intelligent Robots and Systems (IROS)*. IEEE, Maui, Hawaii, USA.

Hammerstad, E., Åsheim, S., Nilsen, K., and Bodhot, H. 1993. Advances in multibeam echo sounder technology. In *Proceedings of the MTS/IEEE Oceans Conference*. IEEE, Victoria, BC, Canada, 1482–1487.

Heidemann, J., Ye, W., Wills, J., Syed, A., and Li, Y. 2006. Research challenges and applications for underwater sensor networking. In *Proceedings of the IEEE Wireless Communications and Networking Conference*. IEEE, Las Vegas, Nevada, USA, 228–235.

Hertzmann, A. 2004. Introduction to bayesian learning. In *SIGGRAPH '04: ACM SIGGRAPH 2004 Course Notes*. ACM, New York, NY, USA, 22.

Jaynes, E. T. 2003. *Probability Theory : The Logic of Science*. Cambridge University Press.

Knight, W., Pridham, R., and Kay, S. 1981. Digital signal processing for sonar. *Proceedings of the IEEE 69,* 11 (Nov.), 1451–1506.

Kuperman, W. A., Hodgkiss, W. S., Song, H. C., Akal, T., Ferla, C., and Jackson, D. R. 1998. Phase conjugation in the ocean: Experimental demonstration of an acoustic time-reversal mirror. *Acoustical Society of America Journal 103*, 25–40.

Li, W. and Preisig, J. 2007. Estimation of rapidly time-varying sparse channels. *IEEE Journal of Oceanic Engineering 32,* 4 (Oct.), 927–939.

Li, Y., Ye, W., and Heidemann, J. 2006. Energy efficient network reconfiguration for mostly-off sensor networks. In *Proceedings of the Third IEEE Conference on Sensor and Adhoc Communication and Networks*. IEEE, Reston, Virginia, USA, 527–535.

Mirza, D., Lu, F., and Schurgers, C. 2009. TB-MAC: Efficient mac-layer broadcast for underwater acoustic sensor networks. In *5th International Conference on Intelligent Sensors, Sensor Networks and Information Processing (ISSNIP)*. 249–254.

Partan, J., Kurose, J., and Levine, B. N. 2006. A survey of practical issues in underwater networks. In *Proceedings of the First ACM International Workshop on UnderWater Networks (WUWNet)*. ACM Press, New York, NY, USA, 17–24.

Polastre, J., Hill, J., and Culler, D. 2004. Versatile low power media access for wireless sensor networks. In *Proceedings of the 2nd ACM Conference on Embedded Networked Sensor Systems (SenSys)*. Baltimore, MD, USA, 95–107.

Preisig, J. 2006. Acoustic propagation considerations for underwater acoustic communications network development. In *Proceedings of the First ACM International Workshop on UnderWater Networks (WUWNet)*. ACM Press, New York, NY, USA, 1–5.

Price, R. and Green, P. 1958. A communication technique for multipath channels. *Proceedings of the Institute of Radio Engineers 46,* 3 (March), 555–570.

Schurgers, C., Tsiatsis, V., and Srivastava, M. B. 2002. STEM: Topology management for energy efficient sensor networks. In *Proceedings of the IEEE Aerospace Conference*. IEEE, Big Sky, Montana, USA, 78–89.

Song, H.-C., Hodgkiss, W. S., and Kuperman, W. A. 2007. MIMO time reversal communications. In *Proceedings of the 2nd ACM International Workshop on UnderWater Networks (WUWNet)*. ACM, New York, NY, USA, 5–10.

Stojanovic, M. 1996. Recent advances in high-speed underwater acoustic communications. *IEEE Journal of Oceanic Engineering 21,* 2 (Apr), 125–136.

Stojanovic, M. 2003. *Wiley Encyclopedia of Telecommunications*. John Wiley & Sons, Inc., Chapter Acoustic (underwater) Communications.

Stojanovic, M., Catipovic, J., and Proakis, J. 1994. Phase coherent digital communications for underwater acoustic channels. *IEEE Journal of Oceanic Engineering 19,* 1 (Jan.), 100–111.

Syed, A., Heidemann, J., and Ye, W. 2010. Managing multipath in underwater acoustic wakeup. Poster at IEEE SECON 2010, Boston, Massachusetts, USA.

Syed, A., Ye, W., Krishnamachari, B., and Heidemann, J. 2007. Understanding spatio-temporal uncertainty in medium access with aloha protocols. In *Proceedings of the Second ACM International Workshop on UnderWater Networks (WUWNet)*. ACM, Montreal, Quebec, Canada.

Syed, A. A., Ye, W., and Heidemann, J. 2008. T-Lohi: A new class of MAC protocols for underwater acoustic sensor networks. In *Proceedings of the IEEE Infocom*. IEEE, Pheonix, AZ, 231–235.

Thrun, S. 1998. Bayesian landmark learning for mobile robot localization. *Machine Learning 33,* 1, 41–76.

Vasilescu, I., Kotay, K., Rus, D., Dunbabin, M., and Corke, P. 2005. Data collection, storage, and retrieval with an underwater sensor network. In *Proceedings of the Third ACM Conference on Embedded Networked Sensor Systems (SenSys)*. ACM Press, New York, NY, USA, 154–165.

Wills, J., Ye, W., and Heidemann, J. 2006. Low-power acoustic modem for dense underwater sensor networks. In *Proceedings of the First ACM International Workshop on UnderWater Networks (WUWNet)*. ACM, Los Angeles, California, USA, 79–85.

Ye, W., Heidemann, J., and Estrin, D. 2004. Medium access control with coordinated adaptive sleeping for wireless sensor networks. *ACM/IEEE Transactions on Networking 12,* 3 (June), 493–506.

Received July 2010; revised December 2011; revised March 2012; accepted March 2012.